The thermo-mechanical behaviour of W-Cu metal matrix composites for fusion heat sink applications: The influence of the Cu content

E. Tejado[1], A. v. Müller[2,3], J-H. You[2], J.Y. Pastor[1]

[1] Departamento de Ciencia de Materiales-CIME, Universidad Politécnica de Madrid

C/ Profesor Aranguren 3, E28040-Madrid, Spain

[2]Max-Planck-Institut für Plasmaphysik, 85748 Garching, Germany

[3]Technische Universität Munchen, 85748 Garching, Germany

CORRESPONDING AUTHOR:

Elena Tejado
Departamento de Ciencia de Materiales-CIME, Universidad Politécnica de Madrid,
C/ Profesor Aranguren 3, E28040-Madrid, Spain.
Telephone: +34 913 365 243
Email: elena.tejado@mater.upm.es

Abstract

Copper and its alloys are used as heat sink materials for next generation fusion devices and will be joined to tungsten as an armour material. However, the joint of W and Cu experiences high thermal stresses when exposed to high heat loads so an interlayer material could effectively ensure the lifetime of the component by reducing the thermal mismatch. Many researchers have published results on the production of W-Cu composites aiming attention at its thermal conductivity; nevertheless, the mechanical performance of these composites remains poor.

This paper reports the characterization of the thermo-mechanical behaviour of W-Cu composites produced via a liquid Cu melt infiltration of porous W preform. This technique was applied to produce composites with 15, 30 and 40 wt% Cu. The microstructure, thermal properties, and mechanical performance were investigated and measured from RT to 800 °C. The results demonstrated that high densification and superior mechanical properties can indeed be achieved via this manufacturing route. The mechanical properties (elastic modulus, fracture toughness, and strength) of the composites show a certain dependency on the Cu content; fracture mode shifts from the dominantly brittle fracture of W particles with constrained deformation of the Cu phase at low Cu content to the predominance of the ductile fracture of Cu when its ratio is higher. Though strong degradation is observed at 800 °C, the mechanical properties at operational temperatures, i.e. below 350 °C, remain rather high—even better than W/Cu materials reported previously.

In addition, we demonstrated that the elastic modulus, and therefore the coefficient of thermal expansion, can be tailored via control of the W skeleton's porosity. As a result, the W-Cu composites presented here would successfully drive away heat produced in the fusion chamber avoiding the mismatch between materials while contributing to the structural support of the system.

1. Introduction

Copper (Cu) and its alloys are used as heat sink materials for next generation fusion devices [1]. To ensure the correct heat transfer of the plasma facing components (PFCs), various combinations of joints between the armour and the heat sink have been developed. Carbon fibre composites were first selected as a plasma facing material for the strike point region of the initial ITER divertor installed for the non-tritium operational phase [2]. However, only tungsten (W) and its alloys are currently considered for the next steps due to its high temperature mechanical properties, low sputtering rate, and low retention of tritium. As a result, the baseline model for the plasma-facing units of the divertor target plates is the ITER-type monoblock design, consisting of an array of tungsten armour monoblocks connected by a copper alloy (CuCrZr) cooling tube [3]. However, recent high heat flux qualification tests [4] and preliminary design studies of the DEMO divertor target predict that CuCrZr could only meet the structural design requirements in a very narrow operation regime [5]. Therefore, advanced heat sink materials need to be developed to improve the divertor target performance.

In addition, the joints between these components must withstand the thermal, mechanical, and neutron loads under cyclic mode of operation while providing high reliability during the lifecycle [6]. However, the joint of W and Cu endures high thermal stresses when exposed to high heat loads due to the great difference in the coefficient of thermal expansion (CTE) and elastic modulus between them [7]. Moreover, the W-Cu system has no mutual solubility and, therefore the bonding strength at the interface is quite low. Functionally graded materials (FGMs) can be used as an interlayer and could effectively reduce the thermal stresses while ensuring the lifetime of the component [8][9]. However, the production of fully dense W-Cu FGMs is not a trivial issue. It is due not only due to these property mismatches, but also due to the great difference between the melting points of W (approximately 3400 °C) and Cu (approximately 1083 °C). This makes it difficult to produce a conventional alloy. To solve this problem, several authors have reported the beneficial effects of cobalt during the sintering process [10] and [11]. The addition of cobalt powder increases the wettability of W particles by Cu by forming an inter-metallic compound Co_7W_6 that reduces the overall porosity in the structure and improves the mechanical properties of the final product [12]. Nonetheless, radioprotection requirements limit the presence of cobalt inside the reactor [13].

Of the preferred methods for producing fully dense W-Cu composites, laser [14] and plasma sintering [15] have gathered much attention in the last few decades. However, these processes are complex, and the problem of adequate electrical conductivity of the powders and the achievement of homogenous temperature distribution is particularly acute [16]. Furthermore, homogeneous and dense W-rich composites (> 60 wt% W) can only be produced by the infiltration technique [17]. In this synthesis route, a W skeleton with desired relative density is produced via powder metallurgy and then compacted and sintered before molten copper is infiltrated into the open pores of the W porous structure [18] [19].

In a previous paper [20], two W-based composites were manufactured with compositions of 30 wt% Cu and 30 wt% CuCrZr with a homogeneous structure and high relative density through the infiltration technique. The results demonstrated that high densification and superior mechanical properties could be achieved through this producing route. In addition, Müller et al. [21] published a preliminary characterization of these W/Cu products. Special focus was given to their thermal conductivity and its suitability as heat sink materials in PFCs for future nuclear fusion devices.

Here, we focused on properly determining the effect of Cu content on the thermomechanical properties including composites with 15 and 40 wt% Cu. The results are compared to those obtained previously for W-30 wt% Cu composites. The microstructure, thermal properties, and mechanical performance were analysed and discussed.

2. Materials and methods

Materials were manufactured in collaboration with Louis Renner GMBH Company (Amtsgericht Stuttgart, Germany) based on the following processing route. Commercial W powders (8 μm) were used to produce a W skeleton consolidated by uniaxial cold pressing. These green specimens were sintered at 1150 °C for 2 h in high purity hydrogen atmosphere and, finally, skeletons with desirable density values, i.e. 85 %, 70 %, and 60 % weight percent (36%, 52%, and 76% pore volume fraction), were infiltrated by oxygen-free molten copper. Infiltration was performed at 1150 °C in hydrogen atmosphere for 2 h. For later characterization, specimens were machined into plates (3 mm x 30 mm x 150 mm). Three different compositions were produced with this technique: W-15 wt% Cu, W-30 wt% Cu and W-40 wt% Cu.

The density of the samples was measured using Archimedes' immersion method in high purity ethanol. The microstructure and fracture surfaces of the composites were characterized by secondary electron microscopy (SEM, ZEISS AURIGA). Energy-dispersive X-ray spectroscopy (EDX) attached in SEM was used to analyse the distribution of the W and Cu components.

From the composite materials, the bend-test (2.8 mm x 2.8 mm x 30.0 mm) and tensile-test (dog bone-shape with 2.0 mm x 2.5 mm x 17.0 mm of narrow portion) specimens were cut. Additionally, bend-test specimens were cut and notched with a femto-second laser for fracture toughness determination (single-edge-laser-notched-beam, SELNB [22]). The mechanical characterization was performed between 25 °C and 800 °C in 125 °C steps under high vacuum ($\sim 10^{-6}$ mBar) with a constant crosshead speed of 100 μm/min. Specimens were heated at 10 °C/min and held at the test temperature for 15 min before testing. The reported values are the average of three measurements.

The bending strength and fracture toughness were obtained in three-point bending configuration with 25 mm span. The yield flexural strength was computed by Bernoulli equations for flexural beams with 0.2 % of deformation. The K_{IQ} was calculated by the general expression of stress intensity factor [23] from the critical load (P_Q) and the beam section. The ASTM 5% secant method [24], i.e. a secant line with a slope equal to 95 % of the initial elastic loading slope of the tangent line, was used to determine P_Q with an

intention to define the K_{IQ} at the 2 % or less crack extension. Apparent values are given here because linear elastic fracture mechanics is not valid when significant plastic deformation precedes failure [25].

Tensile tests were performed on dumbbell or dogbone-shaped samples where the size of the narrow portion of it was 2.0 mm x 2.5 mm x 17.0 mm. This dogbone specimen configuration was chosen so that, during testing, deformation is confined to the narrow centre and, also, to reduce the likelihood of fracture at the ends of the specimen. The output of the tensile tests was recorded as load versus displacement of the frame; these were then normalized to engineering stress and engineering strain. In addition, true stress-strain curves were calculated from the instantaneous cross-sectional area obtained through the non-contact optical full-field Digital Image Correlation (DIC) method.

In order to obtain the instantaneous cross-sectional area, it was necessary to develop a new experimental setup for the recording of the tests. It is important to highlight the limitations of it. Tests were performed inside a high vacuum chamber of significant size (50 cm x 40 cm x 30 cm), operating at temperatures above 800 °C, so any recording system should be outside the chamber and far away from the testing sample. Furthermore, specimens were millimetric, so mounting conventional extensometers, such as strain gages or LVDT (linear variable differential transformer), directly to them is a burdensome task. In addition, painting speckle patterns on the sample surface to facilitate the measurement was insufficient and even useless when testing above 500 °C. So the strain measurements were conducted through the window on the back side of the chamber as validated previously by Zhang [26] on polymeric foam cored sandwich structures, however, the maximum testing temperature achieved by them was 90 °C, which is far below the 800 °C achieved during this work.

The DIC uses image registration algorithms to track the relative displacements of material points between a reference image and a current image; hence, an instantaneous cross-sectional area can be obtained during each test. Constant volume was assumed during the tensile tests. Hence 2D deformation setup was required and only one camera was needed. However, as tests were performed under high temperature and vacuum conditions (30 °C/min heating rate and 10 min dwell time under 10^{-6} mbar pressure), the experimental setup consisted of a high-resolution camera (3840 px x 2748 px) coupled with an adequate light source recording through the window on the back-side of the environmental chamber. To facilitate the DIC measurements, random speckle patterns were painted on the sample surface with a permanent marker. However, at temperatures above 600 °C, only surface roughness with its characteristic grayscale pattern was used to calculate the displacement fields. Prior to the elevated temperature testing, a small mechanical load was applied to verify the symmetry of specimen. Further processing and measurement of the recorded displacement field was performed with the open source 2D DIC MATLAB-based program Ncorr [27]. Once displacement field is obtained, a virtual extensometer was computed in MATLAB to get the instantaneous length, and, thus, instantaneous area, and true strain, from Ncorr records.

The elastic modulus at room temperature was measured on prismatic samples using resonance frequency analysis (RFA). The slope change of the load and load-point displacement curves were used to study the evolution of the elastic modulus with temperature. From these values, we estimated the coefficient of thermal expansion.

3. Results and discussion

The relative densities of the sintered specimens were measured by the Archimedes alcohol immersion method and revealed values of 91.5%, 96.2% and 94.3% for W-15Cu, W-30Cu, and W-40Cu, respectively. These results agree with the ones published by other authors for W-Cu composites produced by the powder injection moulding (relative density of 95.58% with 20% Cu content [28]). However, they are slightly lower than the ones obtained via microwave infiltration sintering method (relative density of 98.87% with 20% Cu content)[29]. However, most researchers have reported the same tendency: with an increasing Cu fraction, internal pores infiltration and Cu migration becomes easier, which makes it easier to fill the pores inside the composite. This increases the density of the final product.

However, most of researchers have reported the same tendency: with an increasing Cu fraction, internal pores infiltration and Cu migration become easier, which makes it easier to fill the pores inside the composite. This increases the density of the final product.

Fig. 1 shows the cross-section microstructure of polished and etched specimens of the W-Cu composites. The EDX mapping analysis shows that the green phase is W, while the surrounding red matrix is Cu. The microstructure shows that polyhedral W grains are distributed in the liquid phase Cu matrix while the solidified liquid phase is intertwined through the solid phase as a network.

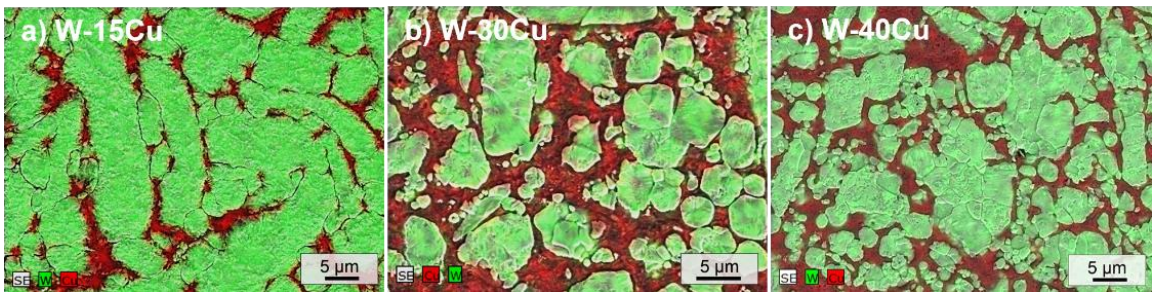

Fig. 1. SEM images with EDX detection of (a)W- 15 wt% Cu, (b)W-30 wt% Cu and (c) W-40 wt% Cu composites after metallographic preparation and etching

On one hand, the difference among the microstructure observed for W-15Cu composite and the others is quite clear. Most of the grains observed at this magnification are W, and hence its average grain size is evidently larger than the observed for the other compounds. On the other hand, no clear differences can be extracted from Fig. 1 b) and c), even though the vol% of Cu is slightly different: 48 vol% Cu and 64 vol% Cu, for W-30Cu and W-40Cu, respectively. In any case, these figures illustrate the contiguity and connective between the W solids, while the Cu-phases are apparently isolated in the matrix of tungsten though this is a continuous phase since it was produced by infiltration over the previous W scaffold. With increasing Cu content, the interconnection of the Cu-phases becomes much more frequent and thus the W–W grains contiguity decreases. Furthermore, the relative density measurements can be confirmed by the absence of visible pores in the Cu matrix.

- *Fracture toughness*

Fracture toughness values of the composites as a function of testing temperature are depicted in Fig. 2. Those data were also compared with literature values for W obtained from [30]. While W-15Cu and W-30Cu exhibited linear elastic load-displacement curves up to the crack onset at RT, the loss of linearity of W-40Cu curves was evident from room temperature and exhibited complex fracture behaviour at elevated temperatures. Since the stress intensity factor loses its validity with increasing ductile behaviour only apparent fracture toughness values are given here.

There is an improvement in the fracture toughness when the Cu content decreases from 40 to 15 wt% (Cu is a weak phase). In addition, a clear trend with temperature can be inferred. The fracture behaviour of W-30Cu and W-40Cu is quite similar with values decreasing constantly with temperature. However, W-30Cu exhibits values on average 30% higher than W-40Cu (16 MPa.m$^{1/2}$ versus 12 MPa.m$^{1/2}$ at 25 °C). Nevertheless, this gap is narrower at high temperature because both composites exhibit almost the same value at 800 °C, 4.9 MPa.m$^{1/2}$ and 6.0 MPa m$^{1/2}$. On the contrary, when the temperature decreases, the effect of the low concentration of Cu (15 wt% Cu) is more evident because it reaches the highest value of fracture toughness at 425 °C, ~ 19 MPa.m$^{1/2}$. The softening of the W grains and the blunting of the crack tip may be the reason of this good mechanical behaviour [31]. Up to this temperature, the Cu ductile phase controls the fracture and, thence the degradation of the composite showing values of around 9 MPa.m$^{1/2}$, which are much higher than the ones observed for the other materials tested. Finally, the difference in toughness between materials at 800 °C is clearly controlled by the percentage of W in the initial skeleton. The toughness increases as the percentage increases.

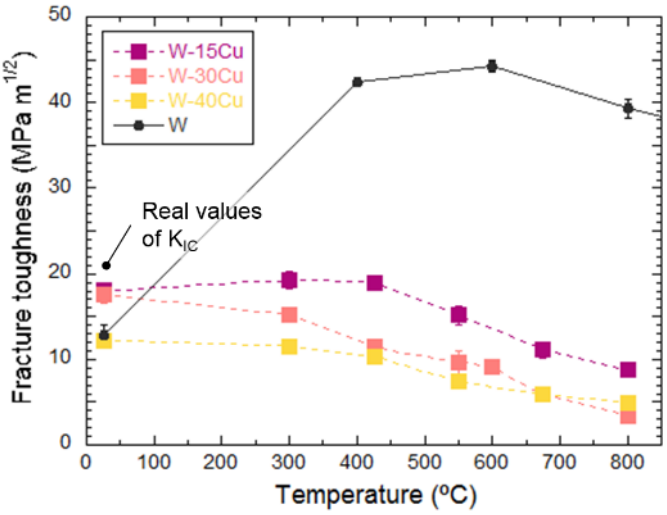

Fig. 2. Apparent fracture toughness of the composites and pure W as a function of temperature and composition. Mean values and standard error

- *Flexural strength*

Fig. 3 shows the variation of flexural strength (0.2 % yield strength) as a function of temperature. The yield strength increases with W content reaching a maximum of 920 MPa at 25 °C when the Cu content is just 15 wt%. Furthermore, the behaviour of the three materials is similar—the bending strength decreases constantly with

temperature with a relative rate of change between 0.55 and 0.70 MPa/°C from 25 °C to 800 °C from 920 MPa to 340 MPa for W-15Cu and from 480 MPa to 120 MPa for W-40Cu. As observed for fracture toughness, the flexural strength of W-30Cu and W-40Cu match closely—especially at high temperatures.

Of note, our results for W-15 wt% Cu materials are much better than the ones reported in the literature for a W-20 wt% Cu composite [32] with a bending strength of almost 800 MPa at 25 °C. In addition, the sintering temperature of those materials, 1250 °C, is beyond the value at 1150 °C for the ones in this study.

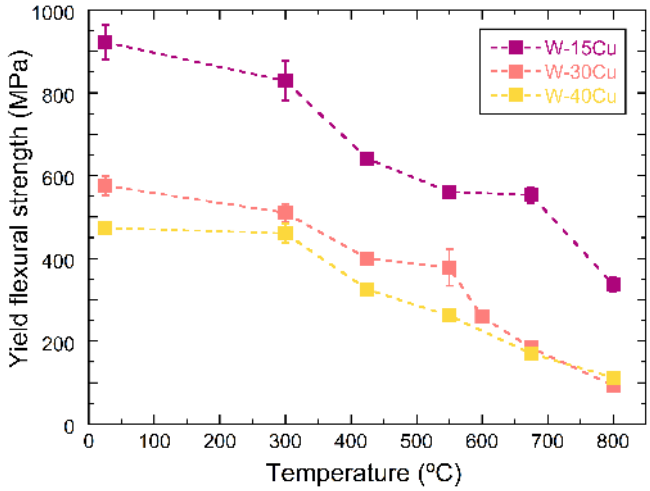

Fig. 3. Yield flexural strength as a function of temperature. Mean values and standard error

- *Tensile strength*

The fracture behaviour of the W-Cu composites can be better observed in Fig. 4 where the true stress-strain curves of the tensile tests are represented. Real displacement as a function of temperature was obtained through DIC analysis with resolutions above 10 µm/pixel. It should be however mentioned that the determination of the elastic displacements is a complex and difficult task, especially for Cu-rich samples where the necessary pre-load may cover this region. Thus, significant imprecisions are expected.

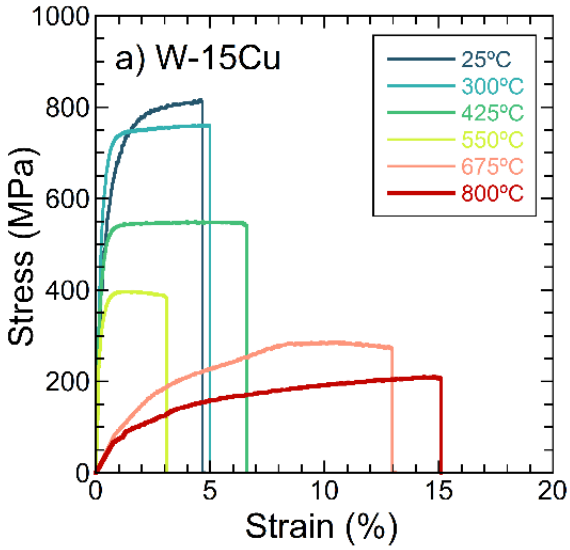

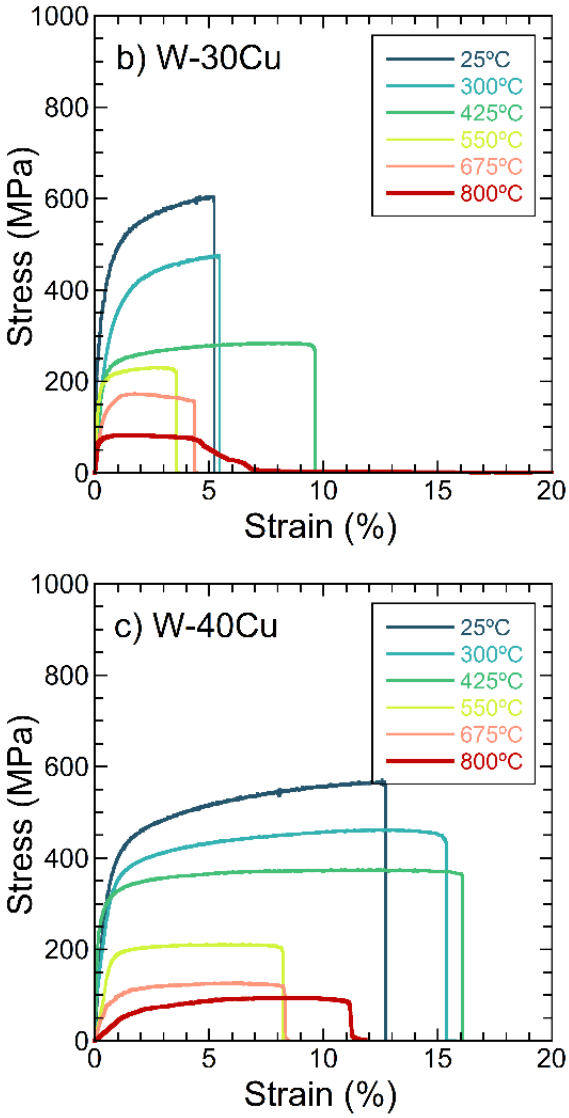

Fig. 4. True stress-strain curves of tensile tests for (a) W-15Cu, (b) W-30Cu and (c) W-40Cu composites at different temperatures

It is noticeable that the addition of Cu leads to a significant increase in ductility, though all materials exhibit ductile behaviour from room temperature. The curves display a characteristic nonlinear behaviour up to fracture after the initial linear region, and the curve shows a substantial nonlinear softening response until fracture occurs. The tensile elongation of W-15Cu composite increases with increasing temperature, while decreasing the true rupture stress excepting for the 550 °C test. However, only one test has been represented for each temperature though average values follow the general tendency observed at remaining temperatures. Zivelonghi [33] explained this scattering in the final rupture strain as a consequence for the random nature of the microstructure of tungsten-reinforced copper composites. On the contrary, both W-30Cu and W-40Cu exhibit utmost rupture strains at 425 °C. At this temperature, the elongation of W-30Cu is indeed twice that exhibited by W-15Cu (~5% strain vs 10% strain) and three times higher in the case of W-40Cu (~15% strain). However, the rupture strength at all temperatures were considerably lower compared to the latter (540 MPa, 380 MPa and 320 MPa at 425 °C for W-15Cu, W-30Cu and W-40Cu, respectively). The tensile strength values can be better

observed in Fig. 5 and Fig. 6 where yield strength at 0.2 % strain and the maximum strength are plotted as a function of temperature and composition.

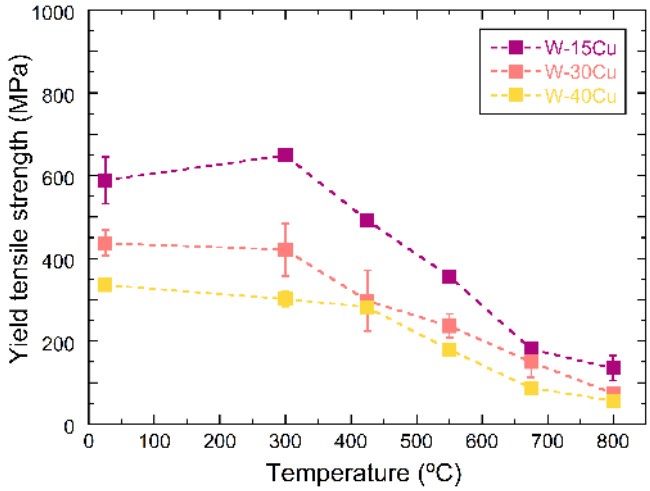

Fig. 5. Yield tensile strength of the composites as a function of composition and temperature

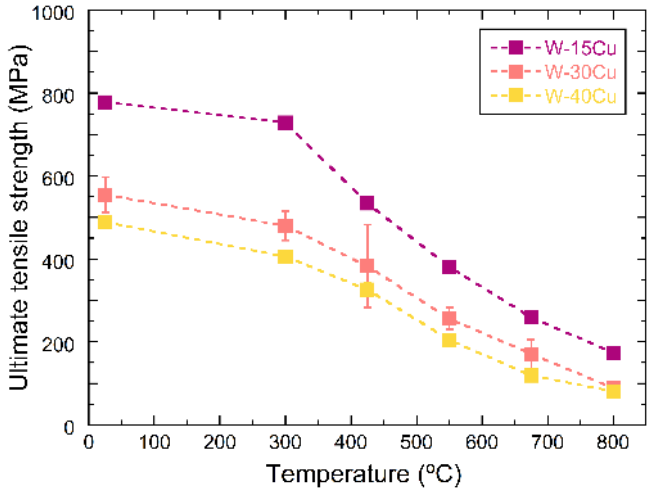

Fig. 6. Maximum tensile strength of the composites as a function of composition and temperature

Both yield and maximum strength show similar trends for the three composites under study. The highest values of tensile strength are obtained at room temperature (780 MPa, 560 MPa, and 500 MPa, for W-15Cu, W-30Cu, and W-40Cu, respectively) and are almost equivalent at 300 °C. Above this temperature, they decrease uniformly down to 175 MPa for W-15Cu and to 80 MPa at 800 °C for W-30Cu and W-40Cu. However, the tensile performance of W-30Cu is on average 18% higher than the observed for W-40Cu, but 40% lower than for W-15Cu. Hence, the effect of Cu content on the tensile behaviour is evident. However, these differences are slightly higher in the case of yield strength (Fig. 5). The onset of plasticity observed at room temperature decreases from 600 MPa to 440 MPa and to 335 MPa as the weight per cent of copper decreases from 15% to 30% to 40%, respectively.

These results agree with the fracture surfaces of the specimens. W-30Cu fractography can be better observed in [20] where a detailed study was performed. Fig. 7 (a-c) show the fracture surfaces of W-15Cu tests at different temperatures. Fig. 7 shows (a) inter- and trans-granular cleavage of W grains (light grey contrast particles) at 25 °C, which indicates

its brittle fracture, while minor deformation of the Cu phase (dark grey contrast phase) can be detected. This is consistent with the rupture strains observed in tensile curves (Fig. 4 (a)).

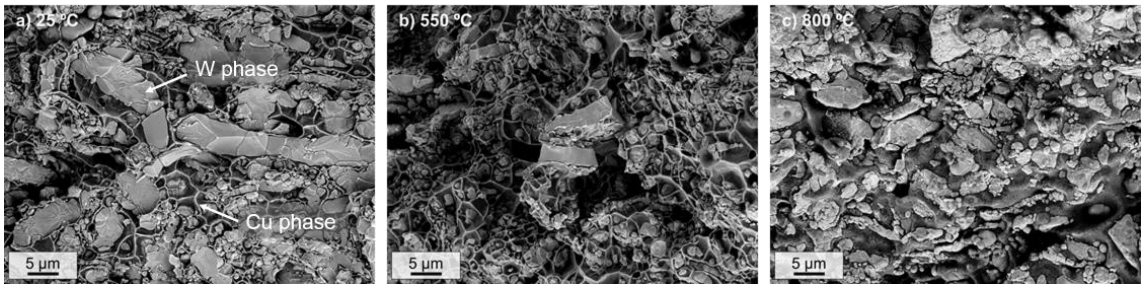

Fig. 7. SEM micrographs of the fractured surfaces of W–15Cu composite tested at a) 25 °C, b) 550 °C, and c) 800 °C

Furthermore, at 300 °C **Error! Reference source not found.** depicts characteristic fan-shaped ridges coming from the origin of the crack inside the grain, thus illustrating the brittle transgranular fracture and cleavage planes inside the grain

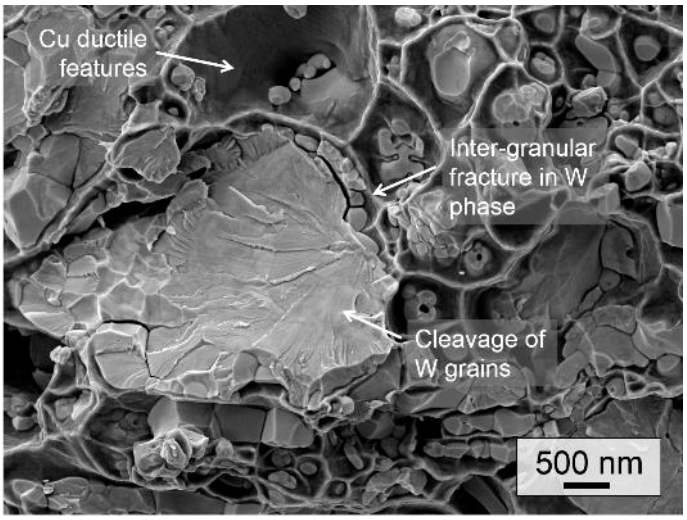

Fig. 8. Fracture surface of W-15Cu composite after tensile testing at 300 °C under vacuum atmosphere

At 550 °C (Fig. 7(b)), some large W residual grains remain; they present a flat fracture surface with cleaved planes, while elongated Cu phase is around them. The effect of Cu on the macroscopic performance increases with temperature. At the maximum temperature under test, the degradation of the material is evident: while W grains are rounded and inter-granular fracture is the dominant mode of rupture in the W skeleton, the viscosity of the Cu phase is reduced as we are close to its melting point (1085 °C). As published by Gaganidze [34], with increasing the test temperature the transition from transgranular cleavage into intergranular fracture in the W skeleton is expected, thus, the fracture energy for the intergranular fracture is about one fourth of the fracture energy for the transgranular cleavage.

The fracture surface of the material containing 40 wt% Cu is quite different compared with the composite containing 15 wt% Cu—especially at 25 °C (Fig. 9 (a)). Contiguity of W particles is rarely observable in contrast with the values observed in the previous

composite. The deformation of the Cu phase is more prominent and particularly visible at 425 °C (Fig. 9 (b)) with the characteristic dimples of a ductile fracture.

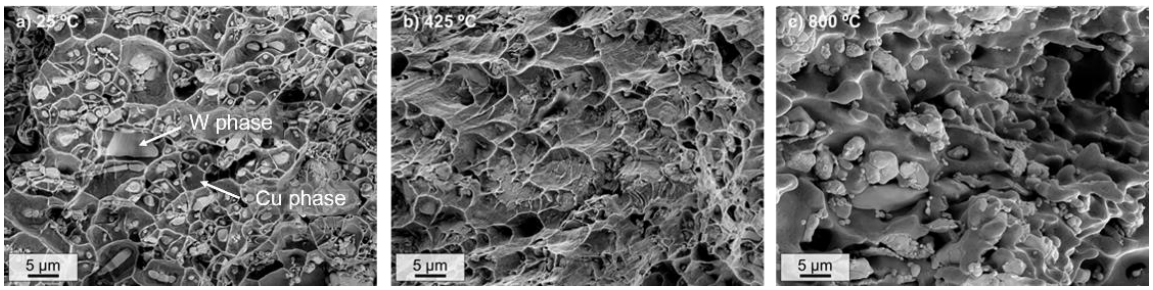

Fig. 9. SEM micrographs of the fractured surfaces of W–40Cu composite tested at (a) 25 °C, (b) 425 °C and (c) 800 °C. Dark particles

- *Elastic modulus*

Load-deflection curves of the tests were used to calculate the modulus of elasticity by drawing a tangent to the steepest initial portion of the straight line. Those data were also compared with literature values for W and Cu obtained from [35] and [36], respectively (Fig. 10).

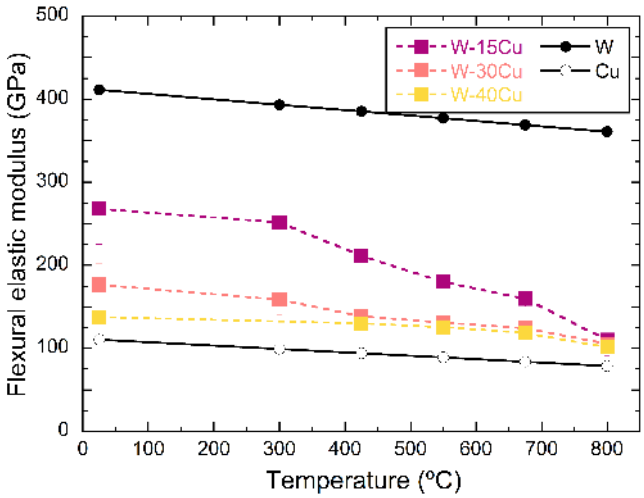

Fig. 10. Elastic modulus of W, Cu, and W–Cu composites as a function of composition and temperature. Figure show mean values and standard error

The evolution of the elastic modulus with temperature for W-40Cu composite is quite similar to the observed for pure Cu with a very small relative rate of change. On the contrary, as Cu content decreases, the difference among the values obtained at RT, where they exhibit the highest, and at 800 °C increases. This is because all the data converge at the same point (~105 GPa). At higher temperatures, the main contribution to the system stiffness comes from the W porous phase because the Cu phase is already degraded.

For a better understanding, the values obtained at RT from the strength tests (ST) have been compared with those obtained via resonance frequency analysis (RFA). Both are represented within the bounds predicted by the rules of mixtures, i.e. Voigt and Reuss models, in Fig. 11.

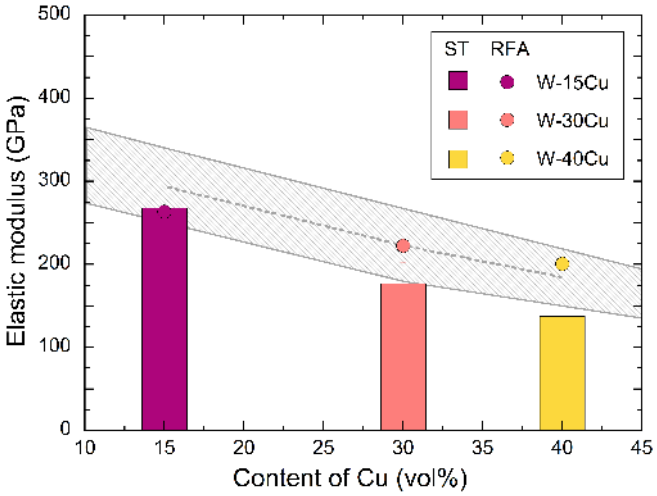

Fig. 11. Elastic modulus at RT of W/Cu composites as a function of composition, mean and standard error. Values were measured from the strength tests (ST) curves and by resonant frequency analysis (RFA). Upper and lower bounds were estimated with the Voigt and Reuss models, respectively, while the Hill model is the average of them

It can be observed that, in all cases, the measured ST data are located between the area limited by the upper and lower bounds represented by the grey area. Furthermore, the data points are systematically closer to the lower bound, i.e. the Reuss model, because the Voigt bound clearly overestimates the stiffness. These data are in good agreement with observed by Hiraoka [37] for W-Cu composites produced by different routes. Totten and MacKenzie [38] explained the Reuss approach of elastic modulus in metal matrix composites by the hydrostatic stresses generated in the composite when the softer matrix phase is restrained from deformation by the hard particles. The elastic modulus values obtained from RFA are significantly higher than those measured from ST when the Cu content is higher than 30 wt%. This observation has already been observed for Cu-based composites [39] and is attributed to the sensitivity of RFA technique to the specimen dimensions and homogeneity [40].

- *Thermal expansion coefficient (CTE)*

Research performed by Arenz [41] found that a large number of polycrystalline and amorphous materials including W and Cu obey the empirical relation $E = 4.5\ \alpha^{-2.3}$, where α is the uniaxial thermal expansion coefficient, and E is the elastic modulus. Both properties are intimately related to the lattice vibration, so the energy well theory and thermodynamic analysis can be used to obtain a qualitative relationship.

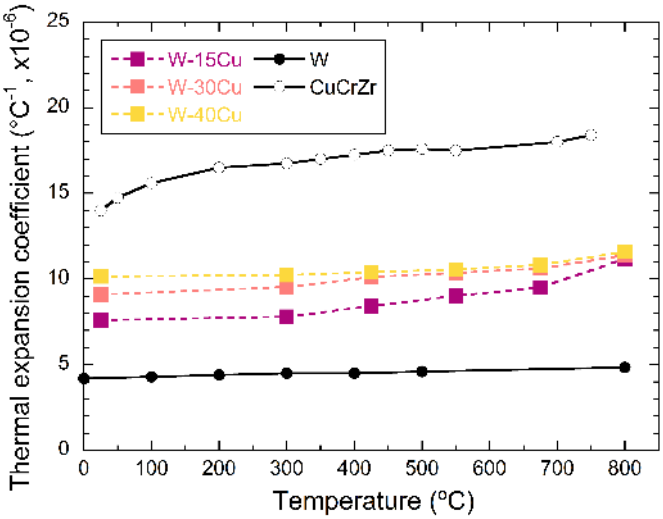

Fig. 12. Estimated coefficient of thermal expansion (CTE) versus temperature for investigated materials

Arenz`s empirical relation was used to estimate the coefficient of thermal expansion (CTE) of the composites under study. The CTE versus temperature for pure tungsten, Cu, and W-Cu composites is illustrated in Fig. 12. The W–Cu composites, either W-15Cu or W-40Cu, show much lower CTE than pure copper. This is higher than that of pure tungsten. As expected, the CTE of W–Cu composites increases with increasing copper content. However, this difference becomes smaller as the temperatures increases.

At room temperature, Duan and coworkers [42] experimentally measured the CTE of W-Cu composites produced by a similar route. Their results agree well with the ones presented in Fig. 12. Furthermore, they treated the CTE of the composites as a weighted average of the thermal expansion of W and Cu in the sample revealing that the variation tendency of measured values of CTE is the same as that of the theoretical ones; hence, the same approach can be done with materials presented in this article.

In W-Cu composites, the high thermal expansion of Cu is constrained by the lower CTE of W particles similar to the elastic modulus. Therefore, the CTE of the composite is affected by the Cu distribution as well as the W-skeleton. At higher temperatures, when Cu is clearly degraded, the CTE is entirely controlled by the W structure. Thus, all the materials tend to have the same value (~ 11.5 x 10^{-6} $°C^{-1}$).

4. Conclusions

W-Cu composites were fabricated via a liquid Cu infiltration of open porous W preforms in an industrially viable production route. Three different compositions have been compared in this investigation: W-15 wt% Cu, W-30 wt% Cu and W-40 wt% Cu.

The resulting microstructure was optimal for heat sink and thermal management applications. It has a high density, a homogeneous distribution of W particles forming a continuous structure, and a Cu phase located around it forming an interpenetrated network structure.

The mechanical properties (elastic modulus, fracture toughness, and strength) of the composites show a palpable dependency on the Cu content. The fracture mode changes from the dominantly brittle fracture of W particles with constrained deformation of the Cu phase at low Cu content (W-15Cu) to the predominance of the ductile fracture of Cu when its ratio is higher (W-40Cu). With increasing temperature, the contribution of the Cu phase to the rupture strain of the materials increases, but strong degradation is observed at 800 °C. Meanwhile, there is no obvious growth of W particles. However, the mechanical properties at operation temperatures, i.e. below 350 °C, remain rather high—even better than other materials reported previously, although slightly lower than the ones reported for W/CuCrZr composites [43]

CTE has been obtained between room temperature and 800 °C from elastic modulus measurements. From these data, it is clear that the W skeleton determined the change in CTE, while the Cu network structure benefits an increase in thermal conductivity as described previously [21]. Furthermore, thermal properties can be tailored by controlling the porosity of the initial W preform; hence, the composition of the final product.

The W-Cu composite materials presented here may be a good candidate for further high heat flux testing. They would successfully drive away heat produced in the fusion chamber avoiding the mismatch between materials by tailoring CTE through the control of W skeleton porosity. Furthermore, these materials exhibit improved mechanical properties that could indeed contribute to the structural support of the system. These facts are of vital importance for enhancing the performance, life cycle, and reliability of the heat sink components.

5. Acknowledgements

This work has been carried out within the framework of the EUROfusion Consortium and has received funding from the Euratom research and training programme 2014-2018 under grant agreement No 633053. The views and opinions expressed herein do not necessarily reflect those of the European Commission.

The authors also acknowledge the support of the Ministerio de Economía y Competitividad of Spain (research project MAT2015-70780-C4-4-P) and the Comunidad de Madrid (research project S2013/MIT-2862-MULTIMATCHALLENGE) who have funded this research.

Bibliography

[1] INTERNATIONAL ATOMIC ENERGY AGENCY, Technical basis for the ITER final design report, cost review and safety analysis (FDR), Vienna, 1998.

[2] G. Pintsuk, V. Casalegno, M. Ferraris, T. Koppitz, M. Salvo, Thermal fatigue characterization of CFC divertor modules using a one step brazing process, J. Nucl. Mater. 426 (2012) 78–84.

[3] J.H. You, E. Visca, C. Bachmann, T. Barrett, F. Crescenzi, M. Fursdon, H. Greuner, D. Guilhem, P. Languille, M. Li, S. McIntosh, A.V. Müller, J. Reiser, M. Richou, M. Rieth, European DEMO divertor target: Operational requirements and material-design

interface, Nucl. Mater. Energy. 9 (2016) 171–176.

[4] H. Greuner, A. Zivelonghi, B. Böswirth, J.H. You, Results of high heat flux testing of W/CuCrZr multilayer composites with percolating microstructure for plasma-facing components, Fusion Eng. Des. 98–99 (2015) 1310–1313.

[5] J.-H.H. You, Copper matrix composites as heat sink materials for water-cooled divertor target, Nucl. Mater. Energy. 5 (2015) 7–18.

[6] V. Barabash, M. Akiba, A. Cardella, I. Mazul, B.C. Odegard Jr, L. Plo, È. Chl, R. Tivey, G. Vieider, Armor and heat sink materials joining technologies development for ITER plasma facing components, J. Nucl. Mater. Volumes 28 (2000) 1248–1252.

[7] J.H. You, H. Bolt, Analytical method for thermal stress analysis of plasma facing materials, J. Nucl. Mater. 299 (2001) 9–19.

[8] G. Pintsuk, S.E. Brünings, J.E. Döring, J. Linke, I. Smid, L. Xue, Development of W/Cu-functionally graded materials, Fusion Eng. Des. 66–68 (2003) 237–240.

[9] Y. Itoh, M. Takahashi, H. Takano, Design of tungsten/copper graded composite for high heat flux components, Fusion Eng. Des. 31 (1987) 279–289.

[10] S.-K. Joo, S.-W. Lee, T.-H. Ihn, Effect of cobalt addition on the liquid-phase sintering of W-Cu prepared by the fluidized bed reduction method, Metall. Mater. Trans. A. 25 (1994) 1575–1578.

[11] I.H. Moon, E.P. Kim, G. Petzow, Full Densification of Loosely Packed W–Cu Composite Powders, Powder Metall. 41 (1998) 51–57.

[12] K. Daneshjou, M. Ahmadi, Optimizing the effective parameters of tungsten - Copper composites, Trans. Can. Soc. Mech. Eng. 30 (2006) 321–327.

[13] V. Barabash, Current status and recent achievements in ITER materials/component fabrication and performance demonstration: vacuum vessel and in-vessel components, in: 16th Intern. Conf. Fusion React. Mater., Beijing, China, 2013: p. 11.

[14] A. Elsayed, W. Li, O.A. El Kady, W.M. Daoush, E.A. Olevsky, R.M. German, Experimental investigations on the synthesis of W-Cu nanocomposite through spark plasma sintering, J. Alloys Compd. 639 (2015) 373–380.

[15] X. Tang, H. Zhang, D. Du, D. Qu, C. Hu, R. Xie, Y. Feng, Fabrication of W–Cu functionally graded material by spark plasma sintering method, Int. J. Refract. Met. Hard Mater. 42 (2014) 193–199.

[16] M. Suarez, A. Fernandez, J.L. Menendez, R. Torrecillas, H. U., J. Hennicke, R. Kirchner, T. Kessel, Challenges and Opportunities for Spark Plasma Sintering: A Key Technology for a New Generation of Materials, in: B. Ertuğ (Ed.), Sinter. Appl., InTech, 2013.

[17] A.G. Hamidi, H. Arabi, S. Rastegari, Tungsten-copper composite production by activated sintering and infiltration, Int. J. Refract. Met. Hard Mater. 29 (2011) 538–541.

[18] J.L. Johnson, J.J. Brezovsky, R.M. German, Effect of liquid content on distortion and rearrangement densification of liquid-phase-sintered W-Cu, Metall. Mater. Trans. A. 36 (2005) 1557–1565.

[19] S. Liang, L. Chen, Z. Yuan, Y. Li, J. Zou, P. Xiao, L. Zhuo, Infiltrated W–Cu composites with combined architecture of hierarchical particulate tungsten and tungsten fibers, Mater. Charact. 110 (2015) 33–38.

[20] E. Tejado, A. v. Müller, J.-H. You, J.Y. Pastor, Evolution of mechanical performance with temperature of W/Cu and W/CuCrZrv composites for fusion heat sink applications, Int. J. Refract. Met. Hard Mater. In press (2017).

[21] A. v. Müller, D. Ewert, A. Galatanu, M. Milwich, R. Neu, J.Y. Pastor, U. Siefken, E. Tejado, J.H. You, Melt infiltrated tungsten–copper composites as advanced heat sink

materials for plasma facing components of future nuclear fusion devices, Fusion Eng. Des. In Press, (2017) 1–5.

[22] T. Palacios, J.Y. Pastor, Influence of the notch root radius on the fracture toughness of brittle metals: Nanostructure tungsten alloy, a case study, Int. J. Refract. Met. Hard Mater. 52 (2015) 44–49.

[23] G. V. Guinea, J.Y. Pastor, J. Planas, M. Elices, Stress Intensity factor, compliance and CMOD for a General Three-Point-Bend Beam, Int. J. Fract. 89 (1998) 103–116.

[24] ASTM Standard E1820-11, Standard Test Method for Measurement of Fracture Toughness, (2009).

[25] A. (Arun) Shukla, Practical fracture mechanics in design, Marcel Dekker, 2005.

[26] S. Zhang, J.M. Dulieu-Barton, R.K. Fruehmann, O.T. Thomsen, A Methodology for Obtaining Material Properties of Polymeric Foam at Elevated Temperatures, Exp. Mech. 52 (2012) 3–15.

[27] J. Blaber, B. Adair, A. Antoniou, Ncorr: Open-Source 2D Digital Image Correlation Matlab Software, Exp. Mech. 55 (2015) 1105–1122.

[28] J. Cheng, L. Wan, Y. Cai, J. Zhu, P. Song, J. Dong, Fabrication of W–20wt.%Cu alloys by powder injection molding, J. Mater. Process. Technol. 210 (2010) 137–142.

[29] L. Xu, M. Yan, Y. Xia, J. Peng, W. Li, L. Zhang, C. Liu, G. Chen, Y. Li, Influence of copper content on the property of Cu-W alloy prepared by microwave vacuum infiltration sintering, J. Alloys Compd. 592 (2014) 202–206.

[30] E. Tejado, Performance of structural materials for the DEMO diverto, Universidad Politécnica de Madrid, 2017.

[31] J. Kübier, Fracture Toughness of Ceramics using the SEVNB Method: From a Preliminary Study to a Standard Test Method, in: Fract. Resist. Test. Monolith. Compos. Brittle Mater., ASTM International, 100 Barr Harbor Drive, PO Box C700, West Conshohocken, PA 19428-2959, 2002: pp. 93-93–14.

[32] A. Ibrahim, M. Abdallah, S.F. Mostafa, A.A. Hegazy, An experimental investigation on the W-Cu composites, Mater. Des. 30 (2009) 1398–1403.

[33] A. Zivelonghi, J.H. You, Mechanism of plastic damage and fracture of a particulate tungsten-reinforced copper composite: A microstructure-based finite element study, Comput. Mater. Sci. 84 (2014) 318–326.

[34] E. Gaganidze, D. Rupp, J. Aktaa, Fracture behaviour of polycrystalline tungsten, J. Nucl. Mater. 446 (2014) 240–245.

[35] J.M. Wheeler, J. Michler, Invited Article: Indenter materials for high temperature nanoindentation, Rev. Sci. Instrum. 84 (2013) 101301.

[36] J.R. Davis, ASM International, Copper and copper alloys, ASM International, 2001.

[37] Y. Hiraoka, T. Inoue, H. Hanado, N. Akiyoshi, Ductile-to-Brittle Transition Characteristics in W–Cu Composites with Increase of Cu Content, Mater. Trans. 46 (2005) 1663–1670.

[38] G.E. Totten, D.S. MacKenzie, Handbook of aluminum, Dekker, 2003.

[39] E. Tejado, M. Dias, C.J. Brito, T. Palacio, P.A. Carvalho, E. Alves, J.Y. Pastor, J.B. Correia, T. Palacios, P.A. Carvalho, E. Alves, J.Y. Pastor, New WC-Cu thermal barriers for fusion applications: high temperature mechanical behavior, J. Nucl. Mater. In press (2017).

[40] M. Radovic, E. Lara-Curzio, L. Riester, Comparison of different experimental techniques for determination of elastic properties of solids, Mater. Sci. Eng. A. 368 (2004) 56–70.

[41] R.J.J. Arenz, Zinc Diffusion in Alpha Brass, Sem. (2005) 1–4.

[42] L. Duan, W. Lin, J. Wang, G. Yang, Thermal properties of W-Cu composites manufactured by copper infiltration into tungsten fiber matrix, Int. J. Refract. Met. Hard Mater. 46 (2014) 96–100.

[43] J.-H.H. You, A. Brendel, S. Nawka, T. Schubert, B. Kieback, Thermal and mechanical properties of infiltrated W/CuCrZr composite materials for functionally graded heat sink application, J. Nucl. Mater. 438 (2013) 1–6.